ELSEVIER

Journal of Crystal Growth 175/176 (1997) 725–729

JOURNAL OF CRYSTAL GROWTH

Growth and characterization of self-organized InSb quantum dots and quantum dashes

T. Utzmeier*, J. Tamayo, P.A. Postigo, R. García, F. Briones

Inst. de Microelectrónica de Madrid, CNM, CSIC, Serrano 144, E-28006 Madrid, Spain

Abstract

We have grown self-organized InSb quantum dots on semi-insulating InP (0 0 1) substrates by molecular beam epitaxy. The size dependency of the uncapped InSb quantum dots on the nominal thickness of the deposited InSb was studied by atomic force microscopy. The dot size has a pronounced minimum at about 2.2 monolayers of InSb. After a nominal thickness of 3.2 monolayers we observe a drastic change of the dot shape, from quantum dots to quantum dashes. From thereon the dots grow in a quasi-cylindric shape aligned in the (1 1 0) direction. The photoluminescence emission of a series of quantum dots was studied, the emission energy being independent of the dot size. When the dots partially relax, the photoluminescence is blue-shifted, which can be explained by a type-II band alignment.

There have been extensive studies on the formation of self-organized quantum-dots (QD) by several growth techniques, such as molecular beam epitaxy (MBE) [1–3], metal-organic chemical vapor deposition [4] and metal-organic vapor-phase deposition [5]. One of the remaining problems of the self-organization of the QDs is the inhomogeneity of the island sizes that broaden the observed PL peaks, and their random distribution over the surface. Also the dot geometry has been studied on (0 0 1) and other surfaces [6].

In this paper we present the growth of InSb QDs on semi-insulating InP (0 0 1) substrates grown by MBE in a pulsed mode, where the group V element is pulsed to enhance the group III surface migration. The self-organized dots were studied by atomic force microscopy (AFM) and photoluminescence measurements. Samples were grown in a conventional solid-source MBE system. After desorption of the InP (0 0 1) oxide at 490°C, we grew a 500 ML thick InP buffer layer, giving a streaky (2×4) reconstruction in the reflection high-energy electron diffraction (RHEED) pattern. Afterwards, the InSb layer was deposited. The surface stoichiometry during growth was controlled by measuring the surface reflection difference signal of the (1 1 0) and (1 − 1 0) directions using a HeNe laser (641.3 nm) at normal incidence to detect the absorption of In-dimers at the growth front reported elsewhere [6]. The InP buffer as well as the InSb islands were grown at a rate of 0.5 ML/s at a growth temperature of 400°C. The growth rate was calibrated by means of RHEED oscillations. After the deposition of 1.2 ML of InSb we observe

* Corresponding author.

PII S0022-0248(97)00816-0

the typical growth mode transition from two-dimensional layer-by-layer growth to three-dimensional island growth, indicated by the onset of a spotty RHEED pattern. This "critical thickness" is very small and it is not quite sure if the islands grow in the Stransky–Krastanow or in the Volmer–Weber mode, i.e. whether they have a wetting-layer or not. During and after the annealing, the samples were kept under Sb flux until the temperature has fallen below 300°C to ensure that no Sb was lost from the surface.

We took atomic force microscope (AFM) images from various spots on each sample, in order to detect a possible inhomogeneity of the dot sizes over the sample. Typical variations of the mean size in different regions of the same sample were less than 15%. The island size and shape of the uncapped QDs were studied by means of AFM. Fig. 1 shows InSb islands of a sample with nominal thickness of 2 ML. The InSb QDs seem to be randomly distributed and have a quite homogeneous size. Their density amounts to 1×10^{10} QDs per cm^2. The size distribution for the dot diameter has a mean value of 24 ± 4 nm. The height distribution has a mean value of 6 ± 3 nm. (The error values given here and in the following refer to standard deviations of the distributions.) We grew further samples from nominal InSb thicknesses of 1.4–2.8 ML. The statistics of these samples can be seen in Fig. 2 (left part). At small nominal InSb thicknesses the dot diameter is about 80 ± 3 nm and decreases strongly with increasing number of InSb monolayers. The dot height is similarly affected by the nominal InSb layer thickness. The dot density shows opposite behavior. As the diameter reaches its minimum at 2.2 ML, the density has a maximum of $4 \times 10^{10}\ cm^{-2}$. After further InSb deposition up to 2.8 ML of InSb, the dot volume rises again, while the density declines. The surprising feature is that the curve in Fig. 2 shows a minimum. The behavior of the dot sizes and density versus the number of InSb monolayers can be explained qualitatively by material exchange processes. At the onset of the 3D growth, when the QD-density is still low, the islands grow more or less independently from each other. Because the mean inter-dot distance diminishes very quickly (about a factor 3 within 0.4 ML) after the first 3D formation, the QDs interact with each other, exchanging material until they reach their optimal

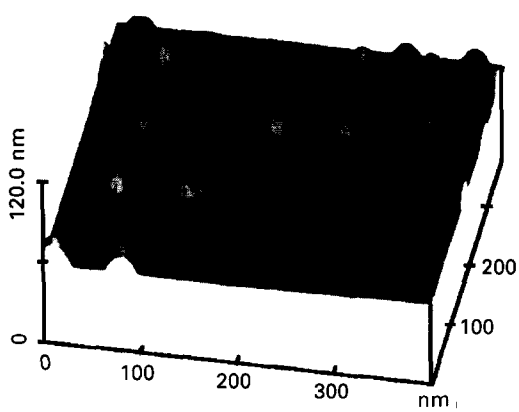

Fig. 1. AFM image of a sample with 2 ML of InSb on InP substrate. The QDs seem to be randomly distributed and have a quite homogenous size. The density amounts to $1 \times 10^{10}\ cm^{-2}$. The mean diameter and height can be seen in Fig. 2.

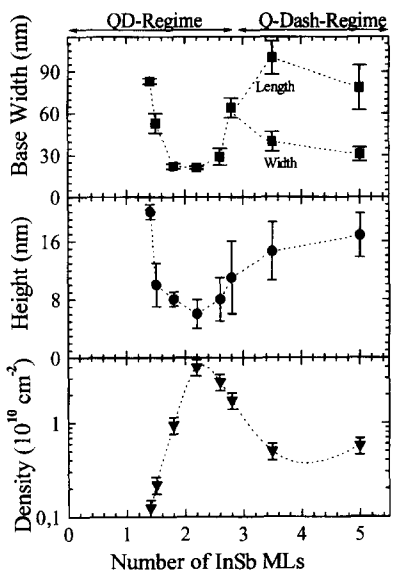

Fig. 2. Statistics on diameters, heights and dot density for various InSb thicknesses. The statistics are made on uncapped samples by AFM. A minimum in size can be observed at around 2.2 ML, where the density is highest. On the right-hand side the quantum dash regime can be seen. Here the islands grow in a quasi-cylindrical shape (see also Fig. 3). The curve for the diameter devides into a curve for length and one for width, respectively. The lines are only a guide for the eye.

size, which is smaller because in this way the surface area is enhanced, which is energetically favorable because this partially relaxes the strain without the formation of dislocations. Similar bahavior has been reported for InAs QDs on GaAs [7, 8]. One has to remember that the samples are grown in an enhanced migration mode. This optimal size seems to be reached at 2.2 ML. Once achieving the optimal size, further InSb deposition results in new island growth, because from then on, the QDs not only interact by material exchange but also through the elastic strain field around each dot (remember the InP substrate next to a QD is expanded) results in a repulsive force between them [9]. Therefore, once having reached the minimum dot distance at 2.2 ML, further deposition can only result in growth of bigger dots, but not more. Furthermore, the density declines with bigger dots because the repulsive force rises with the dot size, which enhances the inter-dot spacing.

If we deposit more than 3.2 ML of InSb we observe a drastic change of the dot geometry (Fig. 3). The QDs no longer have a round shape, but an elongated one. After that point, the QDs maintain their quasi-cylindric shape in all samples with more than 3.2 ML of InSb forming quantum dashes (Q-dash). All Q-dashes are aligned along the (110) direction and their length to width ratio is approximately 2.5. The main Q-dash size is 100 nm long and 40 nm wide, but there are also some bigger ones with length 125 nm and width 66 nm (Fig. 3a). In regions where there is an enhanced surface roughness of the InP substrate, the dots grow all along it. This roughness cannot be explained by the growth conditions because they were the same for all samples (Fig. 1 does not show this roughness), but might be an evidence for an anisotropic strain field due to the Q-dashes, due to the different dimension in length and width. For that reason, we do not believe that the origin of this preferred growth in the (110) direction lies in the surface morphology, but vice versa. Our assumption is supported by the fact that the Q-dashes can grow closer to each other in the lateral than in the longitudinal direction, probably because the repulsive train field in the substrate, originated by the QDs, depends in each direction on the square of the corresponding QD-dimension in that direction. The relative frequencies of the lateral inter-dash spacing w and the longitudinal inter-dash spacing l of the Q-dashes on one sample can be seen in Fig. 4. There are minimum values for w and l of

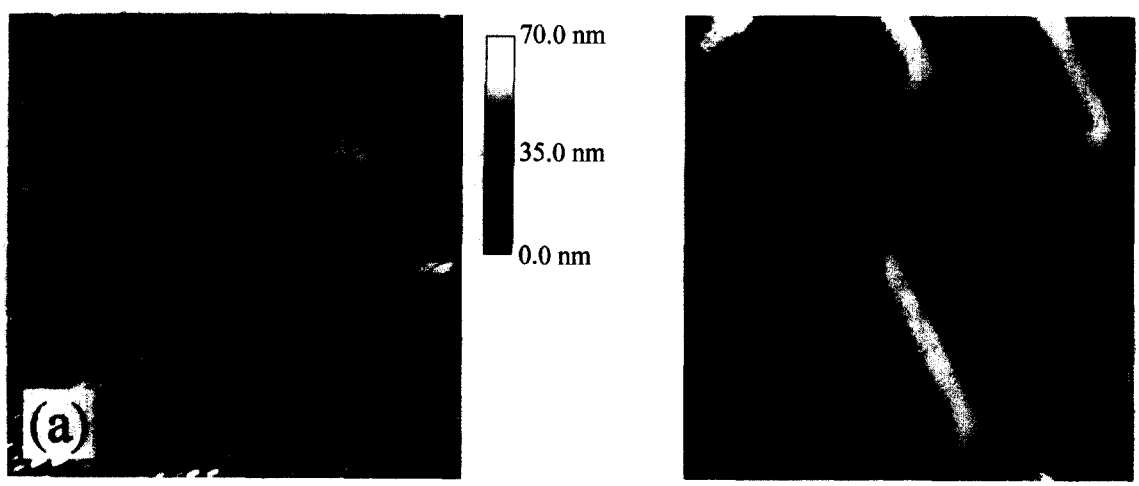

Fig. 3. AFM images of a sample with 3.5 ML of InSb. Image (a) was taken in the height mode, while image (b) was taken in the error signal mode to emphasize the dash edges. The circular QDs have transformed to rectangular quantum dashes. The longer edge lies along the (1 1 0) direction and is about 2.5 times longer than the other one (b). On the left-hand side (a) a higher number of quantum dashes can be seen with dimensions of 100×40 nm, but there are also a few bigger ones, measuring 125×66 nm.

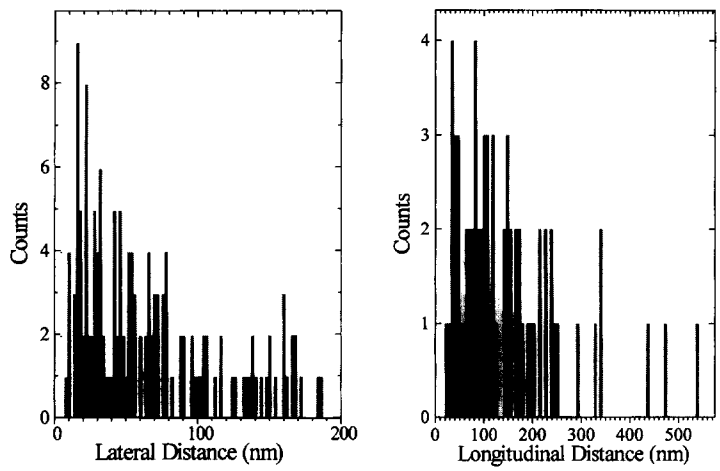

Fig. 4. Statistics on the longitudinal and the lateral spacings between quantum dashes. For the longitudinal distribution we only measured the distance of exactly collinear islands. Both, the longitudinal and the lateral spacings have a minimum value of 23 and 7 nm, respectively.

7 and 23 nm, respectively. The quotient, $l/w = 3.3$, that should depend on the square of the longitudinal and the lateral size of the islands, is somewhat smaller than the theoretical value of 6.3. Assuming an exponential distribution, we obtain a quotient of the mean ranges of the repulsive forces of 2, which is closer to l/w, but the difference to the theoretical value could mean a slight amount of relaxation through dislocations at the interface in the (1 1 0) direction. Only a very small percentage of the Q-dashes are really orientated collinear with others, most of them are displaced with respect to their next neighbors due to the higher strain in that direction, which supports the model of an anisotropic strain field. Thus, the minimum surface energy in the Q-dash regime is obtained with a non-collinear geometry as shown in Fig. 3a. According to Tersoff [10], when the quantum dots pass a critical size, they grow in order to minimize their energy in the dash geometry, as observed in our samples. But his model does not explain why we cannot observe "infinite" large islands instead of many short ones and why the (1 1 0) direction is preferred. Furthermore, we can observe a distribution of the island widths, while the model predicts a constant width. On the other hand, the width distribution is much narrower than the length distribution, suggesting a preferred width value. The constant width in that model is also calculated at constant height, which is probably not the case as seen in Fig. 2, although the error bars are relatively large. Another explanation for the non-constant width could be that wider Q-dashes are formed by two individual ones growing together, which was actually observed on a few occasions on AFM images. In order to understand this unexplained behavior, one has to include the different energies of the different crystal surfaces of the Q-dashes and the interaction of different islands through their strain field in the substrate material.

We studied the photoluminescence of these samples at 12 K, exciting with a Ar^+-laser. The spectra of three samples with 2, 2.8, and 10 ML of InSb dots, respectively, are shown in Fig. 5. The peak at 1.4 eV is attributed to InP, the other two peaks that can be seen at about 1 and 1.2 eV are attributed to two QDs. As more InSb is grown the peak at 1 eV loses intensity, while the one at 1.2 eV gains. Furthermore, the observed blue-shift with growing dot sizes is quite contrary to the expected behavior. The confinement effect of bigger dots should be smaller than that of the smaller ones and therefore a red-shift is expected. But this behavior can be explained supposing a type-II band alignment between the compressed InSb QDs and the InP matrix. Because of the strain applied to the QDs, the InSb

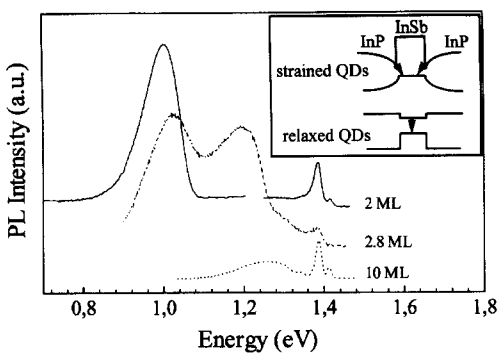

Fig. 5. PL spectra of samples with 2, 2.8 and 10 ML of InSb, respectively. Two peaks at 1 and 1.2 eV can be observed. The one at 1 eV is attributed to strained QDs, while the other one at 1.2 eV is attributed to partially relaxed ones. The inset shows the proposed band alignment for these two cases.

conduction band rises above the InP. On the other side also the InP next to a QDs is expanded, which reduces its band gap in a way that a deep well at the InP/InSb interface is formed in the InP, as seen in the inset of Fig. 5. A type-II alignment has been observed, for example, in GaSb/GaAs QDs [11]. So, when the QD is strained, its emission should be indirect in real space. When the dot reaches a size sufficient to relax, all the strain disappears and a type-I band alignment is obtained again. Therefore, the peak at 1 eV should come from compressed QDs and the other one at 1.2 from partially relaxed ones. In this manner, one can explain why the emission energy of the strained QDs does not shift until about 2.5 ML InSb, although the dot-sizes differ significantly.

The initial stages of growth of InSb QDs on InP substrate have been studied by AFM. typical QD formation can be observed until a InSb thickness of 3.2 ML. From thereon, the quantum-dots drastically change their shape forming Q-dashes along the (110) direction. This behavior can qualitatively be understood, taking into account the elastic energy and surface energy of the QDs and the kinetics of the growth predominantly at the island edges and the repelling force between the islands due to their anisotropic strain field in the substrate. PL measurements of samples with 2–10 ML of InSb reveal that in the strained state, the band alignment between the QDs and the InP matrix material is of type II.

The authors would like to acknowledge the financial support from the European Union (HCM, network CT930349).

References

[1] D. Leonard, M. Krishnamurty, C.M. Reaves, S.P. Denbaar and P.M. Petroff, Appl. Phys. Lett. 63 (1993) 3203.
[2] J.M. Moison, F. Horzay, L. Leprince, E. André and O. Vatel, Appl. Phys. Lett. 64 (1994) 196.
[3] J.-Y. Marzin, J.-M. Gerard, A. Izrael and D. Barrier, Phys. Rev. Lett. 73 (1994) 716.
[4] M. Kimatura, M. Nishioko, J. Oshinowo and Y. Arakawa, Appl. Phys. Lett. 66 (1995) 3663.
[5] R. Nötzel, J. Temmyo, A. Kozen, T. Tamamura, T. Fukui and H. Hasegawa, Appl. Phys. Lett. 66 (1995) 2525.
[6] F. Briones and A. Ruiz, J. Crystal Growth 111 (1991) 194.
[7] J.M. Grárd, J.B. Génin, J. Lefebvre, J.M. Moison, N. Lebouché and F. Marthe, J. Crystal Growth 150 (1995) 351.
[8] A. Ponchet, A. Le Corre, H. L'Haridon, B. Lambert and S. Salaün, Appl. Phys. Lett. 67 (1995) 1850.
[9] L.C.A. Stoop and J.H. Van Der Merwe, J. Crystal Growth 24 (1974) 289.
[10] J. Tersoff and R.M. Tromp, Phys. Rev. Lett. 70 (1993) 2782.
[11] F. Hatami, N.N. Ledentsov, M. Grundmann, J. Böhrer, F. Heinrichsdorf, M. Beer, D. Bimberg, S.S. Ruminov, P. Werner, U. Gösele, J. Heydenreich, U. Richter, S.V. Ivanov, B.Ya. Meltser, P.S. Kop'ev and Zh.I. Alferov, Appl. Phys. Lett. 67 (1995) 656.